ICAS 2016
30th Congress of the International Council of the Aeronautical Sciences
DCC, Daejeon, Korea ; September 25-30, 2016

MODEL PREDICTIVE CONTROL FOR A SWARM OF FIXED WING UAVS

Marco Ariola*, Massimiliano Mattei, Egidio D'Amato**, Immacolata Notaro**, Gaetano Tartaglione***

***Department of Engineering, University of Naples ''Parthenope'', Italy**

****Department of Industrial and Information Engineering, Second University of Naples, Italy**

Keywords: *Cooperative control, formation flight, decentralized MPC, obstacle avoidance*

Abstract

This paper describes an algorithm for the control of a swarm of UAVs based on decentralized MPC. For each UAV, our algorithm first determines the trajectory taking into account the obstacles and the constraints on the aircraft performance. Then basing on a robust MPC algorithm, optimal guidance laws are calculated and tracked by the UAVs by means of local PIDs controllers. Our approach also allows us to take into account moving obstacles and constraints on the minimum distance between the vehicles. Validation of the approach is obtained by means of simulations where for each UAV a 6-DOF model is used.

1 Introduction

Symbols	
$\boldsymbol{I_B}$	Aircraft inertial matrix
$\boldsymbol{I_n}$	Identity matrix of order n
$\boldsymbol{m}$	Aircraft mass
$[\boldsymbol{L}, \boldsymbol{M}, \boldsymbol{N}]^T$	Sum of external moment
$[\boldsymbol{p}, \boldsymbol{q}, \boldsymbol{r}]^T$	Angular speed vector
$[\boldsymbol{u_B}, \boldsymbol{v_B}, \boldsymbol{w_B}]^T$	Speed vector in body fixed frame
$\boldsymbol{V_{TAS}}$	True air speed
$[\boldsymbol{x_E}, \boldsymbol{y_E}, \boldsymbol{z_E}]^T$	Position vector in inertial earth frame
$[\boldsymbol{X}, \boldsymbol{Y}, \boldsymbol{Z}]^T$	Sum of external forces
$\tilde{\boldsymbol{z}}_t$	Reference trajectory point
$\boldsymbol{z}_t$	Actual trajectory point
$\tilde{\boldsymbol{x}}_t$	Reference states
$\hat{\boldsymbol{x}}_{\{t,\dots,t+N\}}$	Optimal state sequence
$\boldsymbol{x}_t$	Actual states
$\tilde{\boldsymbol{u}}_t$	Reference control input
$\hat{\boldsymbol{u}}_{\{t,\dots,t+N\}}$	Optimal control input sequence
$\boldsymbol{u}_t$	Implemented control input
$[\boldsymbol{\phi}, \boldsymbol{\theta}, \boldsymbol{\psi}]^T$	Attitude with respect to the inertial earth frame
$\boldsymbol{\Psi}$	Heading angle

In the recent years, multi-agent cooperative control has been the subject of significant research activity. The interest about this topic is also related to the applications that multi-vehicle systems, such as UAV (Unmanned Aerial Vehicle) fleets, have both in military and civil fields such as intelligence, surveillance, exploration, search and rescue, transportation, monitoring, and so on. In this area, formation flight problems recently have received considerable attention. The main goal of formation flight is to achieve a desired group formation shape while controlling the overall behavior of the group.

Various control schemes have been proposed for UAV formation flight, such as PID control [1], potential method [2],[3],[4],[5], constraint forces [6], adaptive output feedback approaches [7], sliding mode approaches [8], consensus based methods [9],[10],[11], model predictive control (MPC) [12],[13],[14].

In this paper, we will focus on MPC method, which is a feedback control scheme where the control signal is obtained by solving an optimization problem at each sampling time. To calculate the objective and constraint functions, MPC needs to know a reference trajectory and it needs to predict the behavior of the system over a prediction horizon. Although prediction and optimization are performed over a future horizon, only the inputs for the current sampling interval are used. The same procedure is repeated at the subsequent sampling time with

updated measurements and a shifted horizon. On the other hand using a so-called centralized MPC and increasing the number of aircraft in the swarm, the computational cost required for a single optimization can become unsustainable. To solve this problem, the optimization is typically divided into smaller subproblems and, using a decentralized approach (DMPC), each aircraft solves only its own subproblem.

The formation control is based on the so-called $l-\alpha$ theory [15]. We assume that there exists only one formation leader, which conducts the formation to the final position. The position that the followers have to keep from the leader during the flight is expressed by a distance l and an angle α.

The controller is divided in two main parts, characterized by different sampling times: the external control loop and the internal one.

The external control loop, on the basis of the knowledge of the mission goals and the operating environment (obstacle and aircraft positions), computes the aircraft commands in order to follow the reference trajectory. Its architecture relies on a multilayer scheme originally proposed in [16] for general interacting subsystems. In [16] the reference trajectory is generated taking into account the minimum safety distances between the vehicles and obstacles; in this paper we also add operational constraints for a swarm of fixed wing UAVs, such as stall velocity and maximum angular turn rate. A robust DMPC method is then used to compute the reference signal for the PID control system that computes the aircraft commands.

The internal control loop is based on feedback linearization and on a PID control system and it obtains command for the aircraft actuators from the solution of a DMPC method.

To test the controller we consider a fleet of five aircrafts, each one equipped with its own Inertial Measurement Unit (IMU, 3-axes gyros, accelerometers, and magnetometers) and GPS. The dynamics of the aircrafts are simulated by using a 6-DOF model [17] and performance constraints are taken into account.

The papers is organized as follows. In Section 2 we describe the architecture and each part of the formation flight control system. In Section 3 the dynamic model of the aircrafts used to test control algorithms is shown. In Section 4 we describe the scenarios simulated and we show the numerical results. At the end, in Section 5 we draw some conclusions.

Notation: In the sequel by $|\cdot|$ we will denote the Euclidean norm, whereas by $|\cdot|_T$ we will denote the Euclidean norm weighted by the positive definite matrix T. By $A \succ 0$ we mean that each element of the matrix A is greater than 0. The symbol $\wedge$ denotes the cross product between two vectors. The symbols $\oplus$ and $\ominus$ denote respectively the Minkowski sum and the Pontryagin difference [18]. The operator $sign(a)$ returns $+1$ if $a > 0$, -1 if $a < 0$ and 0 if $a = 0$.

2 Formation Flight Control System Architecture

The formation flight control system developed is based on a robust DMPC method; hence each aircraft solves only its own subproblem. As shown in Fig 1, the control system is divided into two main parts with two different sampling times.

The external loop first of all generates the reference trajectory taking into account operational constraints. At each sampling time a new point of the trajectory is calculated solving an LQ optimization problem: the cost function is defined considering the mission goals and the constraints guaranteeing the aircraft performance and minimum safety distances between the vehicles and obstacles. The aircraft inputs needed to track the reference trajectory are calculated by solving another LQ optimization problem, that is introduced in order to implement a robust MPC method. To predict the aircraft behavior, the MPC algorithm makes use of a dynamic model of a material point in a plane, defined in terms of position and heading angle.

The outputs of the external loop are processed by the inner loop to obtain the commands for aircraft actuators. In particular, using the feedback linearization technique we obtain from the MPC outputs the reference speed and heading angle. Eventually a PID

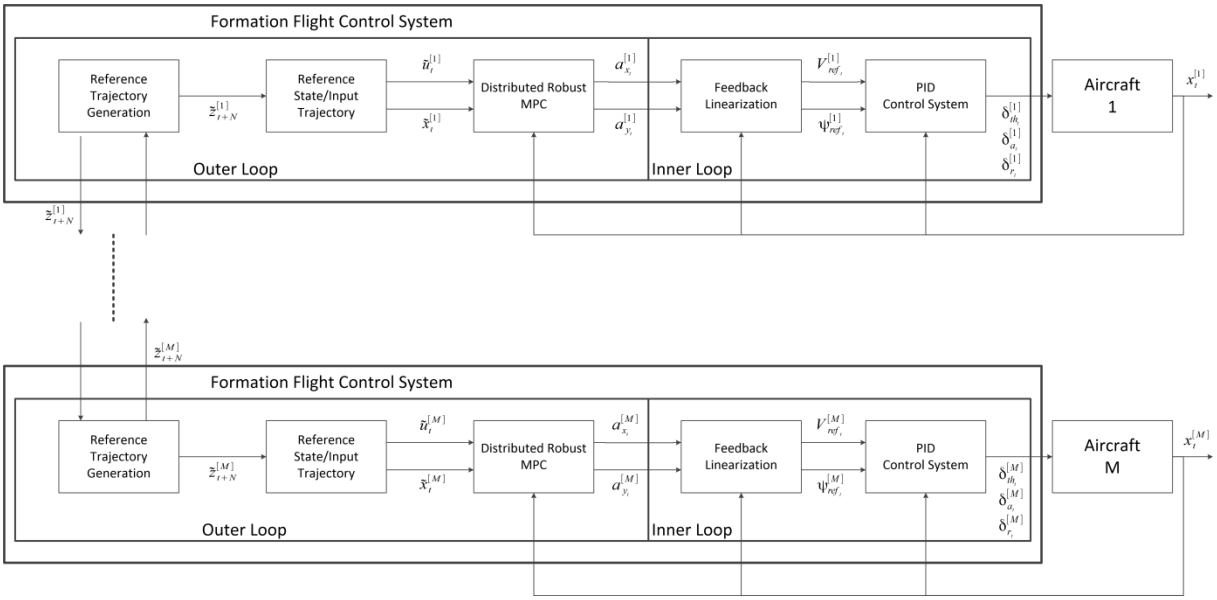

Fig. 1 Formation Flight Control System Architecture

control system computes the actuators command from the reference signal.

3 Reference Trajectory Generation

The MPC algorithm needs to know the reference trajectory over a future horizon of length N to calculate the control input.

The i-th aircraft of the swarm, at time t calculates the next point $\tilde{z}_{t+N}^{[i]}$ of its own trajectory on the basis of the knowledge of the point $\tilde{z}_{t+N-1}^{[i]}$, of the mission goals and of the position of the other aircrafts and obstacles. In particular, $\tilde{z}_{t+N}^{[i]}$ is obtained as the solution of the following constrained optimization problem:

$$\min_{\tilde{z}_{t+N}^{[i]}} L_z^{[i]}$$

$$collision\ avoidance\ constraints; \quad (1a)$$

$$obstacle\ avoidance\ constraints; \quad (1b)$$

$$\tilde{z}_{t+N}^{[i]} \in \mathcal{B}_{t+N}^{[i]}\ ; \quad (1c)$$

$$\tilde{z}_{t+N}^{[i]} \in \mathbb{Z}^{[i]}\ ; \quad (1d)$$

$$formation\ obstacle\ avoidance\ constraints \quad (1e)$$

where, the quadratic cost function $L_z^{[i]}$ guarantees the formation control during the mission and it is based on $l-\alpha$ theory [14]. The form of cost function and the constraints (1a) and (1b) will be discussed in the following sections. Constraint (1c) is included to take into account the aircraft performance (cruise and stall velocity, maximum angular turn rate) and the definition of the set $\mathcal{B}_{t+N}^{[i]}$ will be described in the following sections. Constraint (1d) is added to guarantee that the MPC problem will be feasible and the set $\mathbb{Z}^{[i]}$ depends on the algorithms applied at the lower layer of flight control system. For this reason, the $\mathbb{Z}^{[i]}$ definition will be given in the following section with the description of MPC algorithm.

Finally, constraint (1e) is added only in the optimization problem of leader UAV. The *nominal* position of the followers is only a function of the leader's position and of the geometrical structure of the formation. With constraint (1e) we guarantee that all these nominal positions are outside the regions occupied by the obstacles.

3.1 Definition of cost function for formation flight

The formation control is based on the so-called $l-\alpha$ [14] theory. We consider a swarm of M UAV and we assume that there exists only one

formation leader, for instance aircraft 1. The position that the follower *i* has to keep from the leader during the flight is expressed in terms of both a distance $l^{[i]}$ and an angle $\alpha^{[i]}$ with $i = 2,3,\dots,M$ (see Fig. 2).

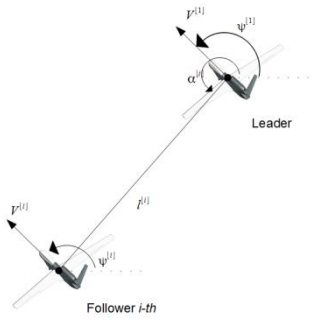

Fig. 2 $l-\alpha$ Formation Control

The leader goal is to conduct the formation to the final position $z^{goal} = \left[x_E^{goal}, y_E^{goal}\right]^T$. Therefore, the cost function of the formation leader is

$$L_z^{[1]} = \gamma \left\| \tilde{z}_{t+N}^{[1]} - \tilde{z}_{t+N-1}^{[1]} \right\|^2 + \left\| \tilde{z}_{t+N}^{[1]} - \tilde{z}^{goal} \right\|_T^2 ; \quad (2)$$

where the weights T and γ are tuning knobs satisfying $T \succ \gamma\, I_2 \succ 0$.

To achieve and hold the formation position, each follower $i = 2,3,\dots,M$ minimizes the following cost function

$$L_z^{[i]} = \gamma \left\| \tilde{z}_{t+N}^{[i]} - \tilde{z}_{t+N-1}^{[i]} \right\|^2 + \left\| \tilde{z}_{t+N}^{[i]} - \tilde{z}_{form}^{[i]} \right\|_T^2 ; \quad (3)$$

where the nominal position $z_{form}^{[i]}$ is defined as

$$\tilde{z}_{form}^{[i]} = \tilde{z}_{t+N-1}^{[1]} + l^{[i]} \begin{bmatrix} \cos\alpha^{[i]} \\ \sin\alpha^{[i]} \end{bmatrix}; \quad (4)$$

In this way, each follower can pursue its own goal knowing the leader position and the formation definition.

3.2 Definition of constraints for obstacle and inner-UAV collision avoidance

To obtain an LQ optimization problem we formulate the obstacle and inner-UAV collision avoidance requirements as linear constraints. We assume that in the operative scenario there exist N_{obs} circular obstacles and the generic *h*-th obstacle is centered at point $z_{obs}^{[h]}$ with radius $R_{obs}^{[h]}$. Denoting by $R^{[i]}$ the radius of the circle circumscribing the *i*-th aircraft, the obstacle avoidance constraint can be formulated as

$$\left\| \tilde{z}_{t+N}^{[i]} - z_{obs}^{[h]} \right\| \geq R^{[i]} + R_{obs}^{[h]} + \delta^{[i]}; \quad (5)$$

where the distance $\delta^{[i]}$ is a safety distance which takes into account the maximum uncertainty about the aircraft position depending on the MPC algorithms. This distance is estimated using the algorithm in [16]. However constraint (5) is nonlinear and non convex, therefore a linear approximation is used. In particular, we use the formulation originally proposed in [19].

We consider a polytope $\mathcal{P}_{obs}^{[hi]}$ with $r_{obs}^{[hi]}$ edges that circumscribes the circle centered at $z_{obs}^{[h]}$ with radius $d^{[hi]} = R_{obs}^{[h]} + R^{[i]} + \delta^{[i]}$ (Fig. 3), its *k*-th edge is defined by the equation $a_k\, x + b_k\, y + 1 = 0$. We introduce the operator

$$\rho_k^{[hi]}(\tilde{z}_{t+N-1}) = -sign(a_k\, x_{obs} + b_k\, y_{obs} + 1) \frac{a_k\, \tilde{x}_{t+N-1}^{[i]} + b_k\, \tilde{y}_{t+N-1}^{[i]} + 1}{\sqrt{a_k^2 + b_k^2}}; \quad (6)$$

in particular, $\rho_k^{[hi]}(\tilde{z}_{t+N-1}) < 0$ if the points $\tilde{z}_{t+N-1}^{[i]}$ and $z_{obs}^{[h]}$ lie at the same side with respect to the line lying on the *k*-th edge of the polytope, otherwise $\rho_k^{[hi]}(\tilde{z}_{t+N-1}) > 0$ and it returns the distance between the point $z_{t+N-1}^{[i]}$ and the line lying on the *k*-th edge of the polytope. To obtain the obstacle avoidance constraint, we select the index $\bar{k}$ corresponding to the maximum value of $\rho_k^{[hi]}(\tilde{z}_{t+N-1})$ and we include in the optimization problem the following linear inequality

$$\rho_{\bar{k}}^{[hi]}(\tilde{z}_{t+N}) > 0; \quad (7)$$

It is worth noting that this *linearization* of the constraint (5) introduces some conservativeness only because the circular region which specifies the obstacle is approximated by a polytope.

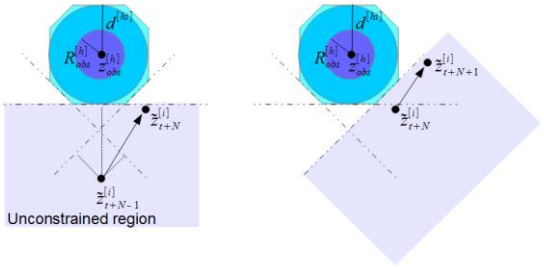

Fig. 3 Linear Approximation for Obstacole Avoidance Constraints

In the similar way it is possible to solve the inter-aircraft collision avoidance problem. The condition that guarantees the collision avoidance between aircraft i and aircraft j with $j = 1,2,\dots,M$ and $j \neq i$ is

$$\left\| \tilde{z}_{t+N}^{[i]} - z_{t+N}^{[j]} \right\| \geq R^{[i]} + R^{[j]} + \delta^{[i]} + \delta^{[j]}; \quad (8)$$

but it is nonlinear and non convex. To solve this problem, we assume that the position $\tilde{z}_{t+N-1}^{[j]}$ is available to aircraft i and we build the polytope $\mathcal{P}_{obs}^{[ji]}$ with $r_{obs}^{[ji]}$ edges that circumscribes the circle centered at $z_{t+N-1}^{[j]}$ with radius $d^{[ji]} = R^{[i]} + R^{[j]} + \delta^{[i]} + \delta^{[j]} + \Delta^{j}$, where Δ^{j} is the maximum distance that aircraft j can cover in one external loop stepping time. At the edges of $\mathcal{P}_{obs}^{[ji]}$ we can apply the operator (6) and obtain the collision constraint linear inequality.

3.3 Definition of constraints for UAV performance

The reference trajectory is defined as a sequence of waypoints satisfying the constraints (1c). To obtain a feasible trajectory, the region $\mathcal{B}_{t+N}^{[i]}$ is built taking into account the aircraft cruise and stall velocity, respectively V_{cruise} and V_{stall}, and the maximum angular turn rate $\dot{\Psi}_{max}$.

Fig. 4 shows how $\mathcal{B}_{t+N}^{[i]}$ is obtained. In particular, the minimum distance and the maximum one between two successive points are defined as

$$d_{min}^{[i]} = V_{stall}^{[i]}\tau;$$

$$d_{max}^{[i]} = V_{cruise}^{[i]}\tau;$$

where τ is the sampling time of the outer control loop. To constrain the maximum angular turn rate, we calculate the direction of the UAV i as

$$\alpha_{t+N-1}^{[i]} = \measuredangle\left(\tilde{z}_{t+N-1}^{[i]} - z_{t+N-2}^{[i]}\right);$$

and the maximum turn angle

$$\Psi_{t+N}^{[i]} = \dot{\Psi}_{max}^{[i]}\,\tau;$$

As shown in Fig. 4, since we want the region $\mathcal{B}_{t+N}^{[i]}$ to be convex, we approximate the arc of the circumference with radius $d_{min}^{[i]}$ with the segment tangent to the circumference.

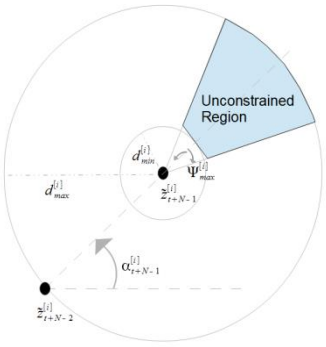

Fig. 4 Set $\mathcal{B}_{t+N}^{[i]}$ definition

4 Distributed robust MPC algorithm

The aircraft control inputs are computed to keep the states and inputs as close as possible to the reference trajectory; they are solution of an LQ optimization problem, that is defined to implement a distributed robust MPC algorithm. Each UAV computes its own control inputs independently from the other vehicles using the same algorithm. Indeed the interaction between the aircrafts has already been considered when calculating the reference trajectories.

In order to predict the aircraft behavior, the MPC algorithm uses as a nominal model a linear approximation of the dynamic model of a material point in a plane. The reference

trajectory is processed by the state/input trajectory layer, in order to obtain the reference trajectory for the states and inputs of the MPC nominal model.

4.1 Definition of nominal model

The MPC algorithm approximates the UAV dynamic with the model of a material point in a plane, defined in terms of position and heading angle:

$$\begin{cases} \dot{x}_E = V\ \cos\Psi \\ \dot{y}_E = V\ \sin\Psi \\ \dot{\Psi} = \omega \\ \dot{V} = a \end{cases} \tag{9}$$

A linear approximation of (9) is obtained with a feedback linearization procedure [15].

Defining $\eta_1 = x_E$, $\eta_2 = \dot{x}_E$, $\eta_3 = y_E$, $\eta_4 = \dot{y}_E$ and introducing the linear accelerations a_x and a_y, we obtain a set of two decoupled double integrators

$$\begin{cases} \dot{\eta}_1 = \eta_2 \\ \dot{\eta}_2 = a\ \cos\Psi - V\omega \sin\Psi \equiv a_x \\ \dot{\eta}_3 = \eta_4 \\ \dot{\eta}_4 = a \sin\Psi + V\omega\ \cos\Psi \equiv a_y \end{cases} \tag{10}$$

We compute a linear approximation of system (9) by means of the following Euler discretization of equation (10) with sampling time τ:

$$x_{t+1} = Ax_t + Bu_t + w_t; \tag{11}$$

$$z_{t+1} = Cx_{t+1}; \tag{12}$$

Where $x_t = \begin{bmatrix} \eta_{1_t} \\ \eta_{2_t} \\ \eta_{3_t} \\ \eta_{4_t} \end{bmatrix}$, $u_t = \begin{bmatrix} a_{x_t} \\ a_{y_t} \end{bmatrix}$, $z_t = \begin{bmatrix} x_{E_t} \\ y_{E_t} \end{bmatrix}$,

$A = \begin{bmatrix} 1 & \tau & 0 & 0 \\ 0 & 1 & 0 & 0 \\ 0 & 0 & 1 & \tau \\ 0 & 0 & 0 & 1 \end{bmatrix}$, $B = \begin{bmatrix} \frac{\tau^2}{2} & 0 \\ \tau & 0 \\ 0 & \frac{\tau^2}{2} \\ 0 & \tau \end{bmatrix}$ and $C = \begin{bmatrix} 1 & 0 & 0 & 0 \\ 0 & 0 & 1 & 0 \end{bmatrix}$. The disturbance w_t has been introduced to model uncertainties and approximation errors of the UAV model and external disturbances. We assume that $w_t \in \mathbb{W}$, where $\mathbb{W}$ is a known bounded uncertainty set. We impose the set of feasible state $x_t \in \mathbb{X}$, where $\mathbb{X}$ is a convex set. It can be readily verified that the triple (A, B, C) is reachable, observable, and does not have invariant zeros in $z = 1$.

4.2 Reference state/input trajectory

The MPC algorithm computes the control input of *i*-th UAV $\boldsymbol{u_t^{[i]}}$ as a solution of an optimization problem defined over a future horizon of N prediction steps. In order to calculate the cost function of the optimization problem, we have to know the reference trajectory for the states and the inputs of the nominal model.

In particular, from the sequence of N geometrical points $\tilde{\boldsymbol{z}}^{[i]}_{\{t,\ldots,t+N-1\}}$ we have to compute the sequence of references states $\tilde{\boldsymbol{x}}^{[i]}_{\{t,\ldots,t+N-1\}}$ and inputs $\tilde{\boldsymbol{u}}^{[i]}_{\{t,\ldots,t+N-1\}}$.

To solve this problem, we implement in the state/input trajectory layer the following dynamic system

$$\begin{bmatrix} \tilde{x}^{[i]}_{t+1} \\ \tilde{e}^{[i]}_{t+1} \end{bmatrix} = \begin{bmatrix} A & 0 \\ -C & I_2 \end{bmatrix} \begin{bmatrix} \tilde{x}^{[i]}_{t} \\ \tilde{e}^{[i]}_{t} \end{bmatrix} + \begin{bmatrix} B \\ 0 \end{bmatrix} \tilde{u}^{[i]}_t + \begin{bmatrix} 0 \\ I_2 \end{bmatrix} \tilde{z}^{[i]}_{t+1} \tag{13}$$

where the new state variable $\boldsymbol{e^{[i]}_{t+1}}$ is the integral of the tracking error $\tilde{z}^{[i]}_{t+1} - C\,\tilde{x}^{[i]}_t$. Given the reachability of the pair (A, B) and the absence of invariant zeros in $z = 1$ of the model (11), it is possible to compute the control law

$$\tilde{u}^{[i]}_t = \tilde{K}_x \tilde{x}^{[i]}_t + \tilde{K}_e \tilde{e}^{[i]}_t \tag{14}$$

where the gain $\tilde{K} = \begin{bmatrix} \tilde{K}_x & \tilde{K}_e \end{bmatrix}$ can be designed with any stabilizing algorithm, such as LQ or pole placement control.

4.3 Definition MPC optimization problem

At each instant the *i*-th UAV solves the following LQ optimization problem to implement the robust MPC algorithm discussed in [16].

$$\min_{\hat{x}_t^{[i]},\hat{u}\_\{t,\dots,t+N-1\}} \sum_{j=0}^{N-1} \left\|\hat{x}_{t+j}^{[i]} - \tilde{x}_{t+j}^{[i]}\right\|_Q^2 + \left\|\hat{u}_{t+j}^{[i]} - \tilde{u}_{t+j}^{[i]}\right\|_R^2 + \left\|\hat{x}_{t+N}^{[i]} - \tilde{x}_{t+N}^{[i]}\right\|_P^2$$

$$\hat{x}_{t+1}^{[i]} = A\hat{x}_t^{[i]} + B\hat{u}_t^{[i]} \quad (15a)$$

$$\hat{x}_{t+j} \in \hat{\mathbb{X}}^{[i]}, \ \ \forall j = 1, \dots, N-1 \quad (15b)$$

$$x_t^{[i]} - \hat{x}_t^{[i]} \in \varepsilon^{[i]} \quad (15c)$$

$$C\left(\hat{x}_{t+j}^{[i]} - \tilde{x}_{t+j}^{[i]}\right) \in \Delta_z^{[i]} \ \ \forall j = 1, \dots, N-1 ; \quad (15d)$$

$$\tilde{x}_t^{[i]} - \hat{x}_t^{[i]} \in \kappa^{[i]}\varepsilon^{[i]} \quad (15e)$$

The set $\varepsilon^{[i]}$ in (15c is defined as the robust positively invariant (RPI) set

$$\varepsilon^{[i]} = \oplus_{j=0}^{\infty} (A + BK)^j \mathbb{W}^{[i]} \quad (16)$$

where the gain K must be defined so as to obtain $(A + BK)$ to be Schur stable. Methods for computing approximation of (16) are discussed in [23]. The set $\hat{\mathbb{X}}^{[i]}$ in (15b) is computed as

$$\hat{\mathbb{X}}^{[i]} = \mathbb{X}^{[i]} \ominus \varepsilon^{[i]} \quad (17)$$

The set $\Delta_z^{[i]} \subseteq \mathbb{R}^2$ in (15d) is characterized by a trade-off: a small size of this parameter permits only small deviations of the nominal state trajectory with respect to the reference one, but it can have the effect of limiting the robustness of the control scheme. Finally, $\kappa^{[i]} > 0$ in (15e is a tuning parameter.

In the functional cost, the symmetric weighting matrices $Q \geq 0$ and $R > 0$ are free design parameters, while P is assumed to satisfy the Lyapunov equation

$$(A + BK)^T P(A + BK) - P = -(Q + K^T RK) \quad (18)$$

The input controls for the i-th aircraft are calculated from the solution of the optimization above problem as

$$u_t^{[i]} = \hat{u}_{t|t}^{[i]} + K(x_t^{[i]} - \hat{x}_t^{[i]}) \quad (19)$$

5. Inner control loop

In order to track the reference trajectory, the inner control loop computes the command input for the aircraft actuators from the input controls calculated by the MPC algorithm. It is characterized by a sampling time smaller than the outer loop $\boldsymbol{\tau_{in}} \ll \boldsymbol{\tau}$ and two main parts: the feedback linearization procedure and a PID control system.

The feedback linearization procedure allows us to calculate the speed reference $\tilde{\boldsymbol{V}}_{\boldsymbol{t+1}}^{[\boldsymbol{i}]}$ and the heading angle reference $\tilde{\boldsymbol{\Psi}}_{\boldsymbol{t+1}}^{[\boldsymbol{i}]}$ from the linear accelerations obtained by the MPC algorithm. In particular, using the definition of $\boldsymbol{a}_{\boldsymbol{x}}^{[\boldsymbol{i}]}$ and $\boldsymbol{a}_{\boldsymbol{y}}^{[\boldsymbol{i}]}$ in (10) and the knowledge of the true air speed $\boldsymbol{V}_{\boldsymbol{t}}^{[\boldsymbol{i}]}$ and heading angle $\boldsymbol{\Psi}_{\boldsymbol{t}}^{[\boldsymbol{i}]}$, we obtain

$$\tilde{V}_{t+1}^{[i]} = V_t^{[i]} + \tau_{in}\left(a_x^{[i]} \cos\Psi_t^{[i]} + a_y^{[i]} \sin\Psi_t^{[i]}\right); \quad (20a)$$

$$\Psi_{t+1}^{[i]} = \Psi_t^{[i]} + \frac{\tau_{in}}{V_t^{[i]}}\left(-a_y^{[i]} \sin\Psi_t^{[i]} + a_y^{[i]} \cos\Psi_t^{[i]}\right); \quad (20b)$$

Finally, the command signals for the aircraft actuator are computed by a PID control system (see Fig. 5). In particular, the speed control system computes the thrust needed to control the true air speed. The aircraft changes the heading angle performing a coordinated turn. For this reason, the heading control system calculates the reference roll angle, that is used by the roll-attitude hold to obtain the aileron command. To maintain zero sideslip angle, a sideslip control and yaw dumper system are implemented and they compute the rudder command. The PID control system includes also an altitude control system to maintain constant

the altitude during the mission. It calculates the reference pitch angle, that is used by the pitch-attitude hold to obtain the elevator command.

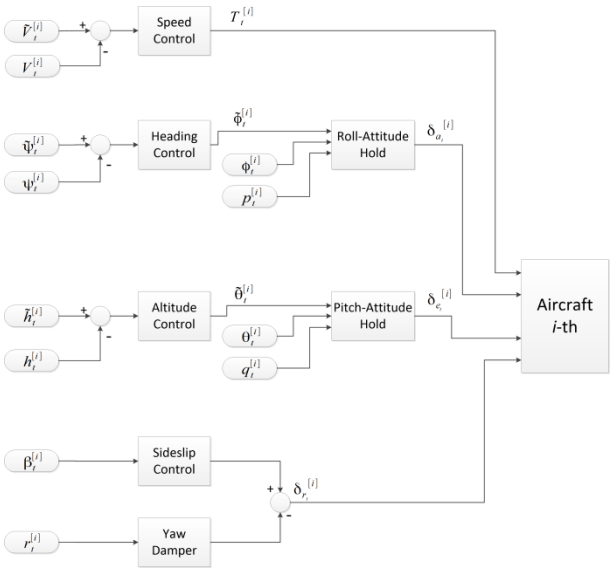

Fig. 5 PID control system

6. Numerical simulations

To test the controller we considered a fleet of five aircrafts, each one equipped with its own Inertial Measurement Unit (IMU, 3-axes gyros, accelerometers, and magnetometers) and GPS.

We considered tactical uninhabited vehicles primarily intended for medium endurance and short range surveillance, reconnaissance and patrolling missions. Each aircraft is powered by one pusher propeller located at the end of the fuselage. The principal features of the UAV configuration are: high aspect ratio, tapered, untwisted, high mounted wing with no dihedral, high horizontal tail, double vertical tail with double rudder and cylindrical fuselage. Aircraft main parameters can be found in Table 1.

Parameter	Value
Length	2.13m
Height	0.570m
Wing Span	3.162m
Aspect Ratio	10
Wing Area	1.0m2
Maximum Take Off Weight	29kg
Payload	10kg
Operational Radius	50Nmi
Loitering Time	2hrs
Max Cruise Speed	90kts
Max Cruise Altitude	5000m

Table 1 Aircraft main parameters

The UAV mathematical model is obtained from the nonlinear six degree of freedom model and the aerodynamic forces and moments are obtained considering a linear aerodynamic model of the UAV. In particular, the stability and control derivatives were calculated using a statistical approach [20],[21],[22].

The controller performance are tested in simulation in a scenario with two circular obstacles characterized by $R_{obs}^{[i]} = 500m$ with $i = 1,2$. The shape formation is designed by the following parameters

$$l^{[2]} = 100m \qquad \alpha^{[2]} = 135deg$$

$$l^{[3]} = 100m \qquad \alpha^{[3]} = 135deg$$

$$l^{[4]} = 100m \qquad \alpha^{[4]} = -135deg$$

$$l^{[5]} = 200m \qquad \alpha^{[5]} = -135deg$$

At the beginning of the simulation the followers positions are random, so their first goal is to reach the leader and achieve the formation. Meanwhile, the leader flies to its position goal avoiding the obstacles.

The numerical results are shown in the following figures. In Fig. 6a we show the reference trajectories computed by the Reference Trajectory Generation layer while in Figure 6b we show the trajectories carried out by the aircrafts.

The tracking error of the flight control system can be analyzed by overlaying the curves: for instance in Fig. 7 we compare the reference and actual trajectory of UAV #1.

Despite the tracking error, the collision avoidance constraints are respected. The Fig. 8a and 8b show that the no-fly zone are not violated and Fig. 8c shows that the minimum safety distances between leader and followers are respected.

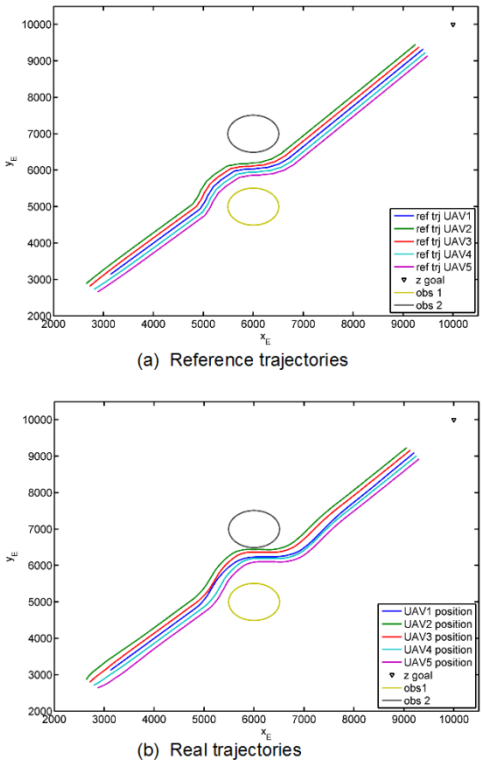

Fig. 6 Aircraft trajectories

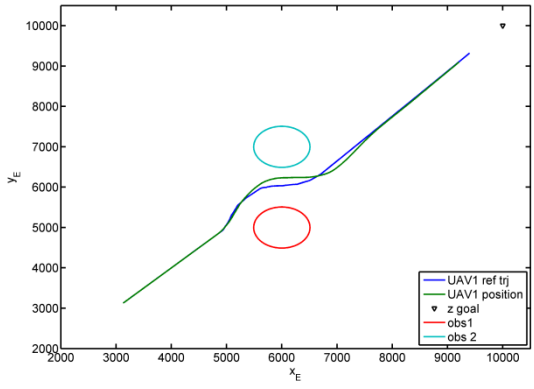

Fig. 7 Comparison Aircraft 1 trajectories

Finally, to verify that during the mission the aircraft real position reach the shape formation, we introduce the following error index

$$E_t^{[i]} = \left\| z_t^{[i]} - z_t^{[1]} - l^{[i]} \begin{bmatrix} \cos\alpha^{[i]} \\ \sin\alpha^{[i]} \end{bmatrix} \right\| \qquad (21)$$

Fig. 9 shows that before and after the obstacles the error indices decrease because the aircrafts are composing the formation. Because of the maneuvers to avoid the obstacles the formation is broken and the indices increase.

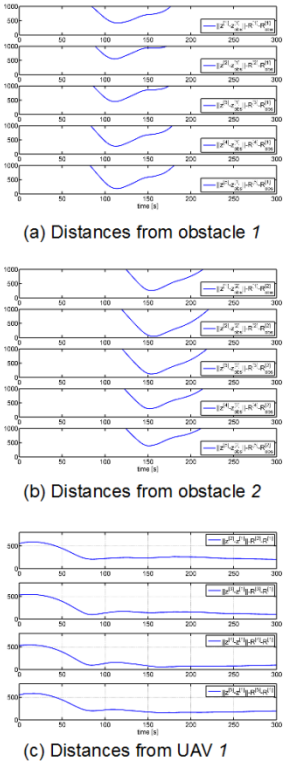

Fig. 7 Verification collision avoidance constraints

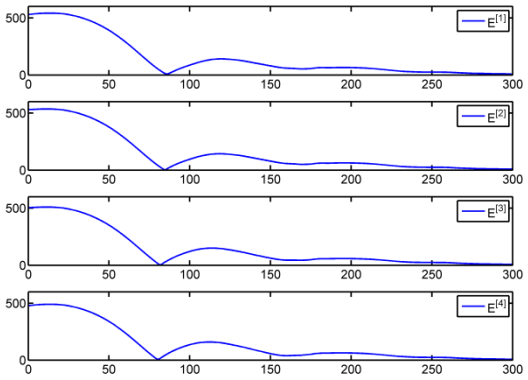

Fig. 8 Error indices

7. Conclusions

In this paper, an algorithm for the control of a swarm of UAVs based on decentralized MPC has been proposed. The first step of the algorithm consists of the calculation of the trajectory of each UAV so as to take into account the obstacles and the constraints on the

aircraft performance. Then optimal guidance laws are calculated based on a robust MPC algorithm. Some numerical simulations show the effectiveness of the proposed approach.

References

[1] Lou D, Xu W and Wu S. *UAV formation flight control and formation switch strategy*. The 8th International Conference on Computer Science & Education, Colombo, Sri Lanka, pp 264-269, 2013. Publisher, 2001.

[2] Paul T, Krogstad T R and Gravdahl J T. *UAV Formation Flight using 3D Potential Field*. Proc 16th Mediterranean Conference on Control and Automation, France, 2008.

[3] Suzuki U K M. *Three-Dimensional Formation Flying Using Bifurcating Potential Fields*, Proc AIAA Guidance, Navigation, and Control Conference, Chicago, Illinois, 2009.

[4] Vanualailai J, Sharan A and Sharma B A. *A swarm model for planar formations of multiple autonomous unmanned aerial vehicles*, Proc IEEE International Symposium on Intelligent Control, pp 206-211, 2013.

[5] Garcia-Delgaro L, Dzul A, Santibanez V and Llama M. *A swarm model for planar formations of multiple autonomous unmanned aerial vehicles*, Proc IEEE International Symposium on Intelligent Control, pp 206-211, 2013.

[6] Zou Y and Pagilla P R. *Distributed Formation Flight Control Using Constraint Forces*, Journal of Guidance, Control, And Dynamics, Vol. 32, pp 112-120,2009.

[7] Sattigeri R and Calise A J. *Adaptive Vision-based Approach to Decentralized Formation Control*, AIAA Guidance, Navigation, and Control Conference, Rhode Island, 2004.

[8] Galzi D and Shtessel Y. *UAV formations control using high order sliding modes*, Proc American Control Conference, Minneapolis, 2006.

[9] Ren W. *Leaderless Formation Control for Multiple Autonomous Vehicles*, Proc AIAA Guidance, Navigation, and Control Conference, Colorado,2006.

[10] Kuriki Y and Namerikawa T, *Consensus-based cooperative control for geometric configuration of UAVs flying in formation*, Proc SICE Annual Conference, pp 1237-1242, 2013.

[11] Dong X, Yu B, Shi Z and Zhong Y. *Time-Varying Formation Control for Unmanned Aerial Vehicles: Theories and Applications*, IEEE Transactions on Control Systems Technology, Vol. 23, No. 1, pp 340-348, 2014.

[12] Richards A and How J. *Decentralized model predictive control of cooperating UAVs*, Proc 43th IEEE Conference on Decision and Control, Vol. 4, pp 4286-4291, 2004.

[13] Zao W and Go T H, *Quadcopter Formation Flight Control Combining MPC and Robust Feedback Linearization*, Journal of the Franklin Institute, Vol. 351, No. 3, pp 1335-1355, 2014.

[14] Fierro R, Das A K, Kumar V and Ostrowski J P. *Hybrid control of formation of robot*, International Conference on Robotics and Automation,pp 157-162, 2001.

[15] Oriolo G, De Luca A and Vendittelli M. *WMR control via dynamic feedback linearization: design, implementation, and experimental validation*, IEEE Trans. Control Syst. Technol., Vol 10, No. 6, pp 835-852, 2002.

[16] Farina M, Betti G, Giulioni L, Scattolini R, An approach to distributed predictive control for tracking - theory and application, IEEE Trans. Control Syst.Technol., Vol 22, No. 4, pp 1558-1566, 2014.

[17] Stevens B L and Lewis F L, *Aircraft Control and Simulation*, 2nd Edition, 2003.

[18] Nguyen H N, *Constrained Control of Uncertain, Time-Varying, Discrete-Time Systems: An Interpolation-Based Approach*, Springer, 2013.

[19] Farina M, Perizzato A, Scattolini R. *Application of distributed predictive control to motion and coordination problems for unicycle autonomous robots*, Robotics and Autonomous Systems, Vol 72, pp 248-260, 2015.

[20] Roskam J. *Airplane Design (Part I-VIII)*, DAR Corporation, Lawrence, Kansas, 1990.

[21] Raymer D P, *Aircraft Design: A Conceptual Approach*, AIAA Education Series, 2006.

[22] McCormick B W. *Aerodynamics, Aeronautics, and Flight Mechanics*, John Wiley and Sons, New York.

[23] Rakovic S V, Kerrigan E C, Kouramas K I, Mayne D Q. *Invariant approximation of the minimal robust positively invariant set*, IEEE Trans. Automat. Control, Vol 50, No. 3, pp 406-410, 2005 .

Contact Author Email Address

marco.ariola@uniparthenope.it

Copyright Statement